Fatigue 2010

# Influence of ply-drop location on the fatigue behaviour of tapered composites laminates

A. Weiss[1], W. Trabelsi[1], L. Michel[1]*, J.J. Barrau[1] and S. Mahdi[2]

[1]*Université de Toulouse ; INSA,UPS, Mines Albi, ISAE, ICA (Institut Clément Ader), 10 avenue Edouard Belin -BP 54032 - F-31055 Toulouse cedex 4*
[2] *Airbus Operations SAS, 316, Route de Bayonne, F-31060 Toulouse Cedex 03*

**Abstract**

The influence of ply-drop position in thickness direction under fatigue loading (R = -1) has been studied for a highly oriented composite laminate dropping from 20 to 12 plies. Compressive and tensile strengths have been determined for several configurations of ply-drop locations. Fatigue tests at a load ratio of R=-1 have been performed up to rupture. The first damages clearly identified are delaminations close to the drop-offs. Their initial locations and propagations kinetics before final failure were observed. Finite element simulations were performed to find out initiation spots of delamination. An interlaminar stress criterion has been proposed to predict initiation of delaminations. Effects of ply-drops configuration on fatigue are discussed.

*Keywords: ply*-drop, fatigue, damage modes, numerical simulation, composite

## 1. Introduction

Modern aeronautical structures are being made of laminated composites panels, i.e. several Carbon-Fibre Reinforced Plastic plies stacked together. In order to optimise the structure weight, the thickness of the panel can be tailored to the local stress distribution. These thickness variations may be efficiently produced by so-called ply drop-offs. In these zones, however, out of plane stress concentrations are susceptible to initiate delamination failures. This being a critical failure mode, several studies have been carried out about damage and delamination propagation in these ply drop areas [1,3,4,6]. Design guidelines have been proposed to avoid, or minimise, damage initiation for simple specimen geometry, i.e. with one or two ply drops [2,5]. These studies give basic ideas about the influence of ply-drops on static and fatigue load behaviours. The present study goes further by addressing the fatigue behaviour of specimens with several ply-drop offs configurations defined to meet the aeronautical industry design guidelines.

The objective of the study is then to evaluate the effect of variations in ply-drop positions on the fatigue resistance of representative specimens. To do so, several ply-drop configurations have been defined and tested under

* Corresponding author. Tel.: +0-33561339141; fax: +0-33561339095.
*E-mail address*: laurent.michel@isae.fr.

static (tension and compression) and monotonic fatigue loading. For fatigue, the load ratio was fixed to R=-1, that is considered to be the most critical one for composite specimens. Damage initiations, as well as damage evolutions before final failure, were observed during fatigue mechanical tests in order to explain the differences in fatigue lifetime of the different configurations. 3D Finite Element Models were developed to estimate the interlaminar stresses close to the ply-drop locations. The locations of delamination initiation, observed experimentally in fatigue, are analysed with the help of these numerical models. An interlaminar stress criterion is evaluated to estimate the static results obtained in compression. The SN curves are then presented and ply-drop configuration effects are discussed.

## 2. Experiments

### *2.1. Material, Stacking sequence and dimensions of the ply-drop specimens*

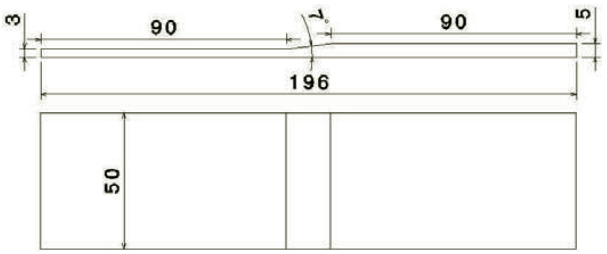


Fig. 1. Geometry of ply-drop specimen

The material is a pre-impregnated carbon /epoxy composite from Hexcel (T700-M21, 268 g/m$^2$), the thickness of the unidirectional plies is 0.25 mm. The ply-drop zone is non symmetrical with an angle of 7°, as may be seen in Fig. 1. In the tapered area, the plies are dropped, from 20 to 12 plies, by respecting the typical design guidelines for ply-drop-offs. The thick and thin sections of the laminates are strongly oriented, with 50% of the plies at 0°. Both sections and the dropped plies are the same for all configurations (Fig. 2.). Six configurations of ply-drop offs were defined to study the effect of ply-drop location in the thickness of the specimen on its mechanical behaviour. For convenience and as the first two ply-drops close to the thin section were observed as being the most critical for damage initiation, only the position of these ply-drops is presented in Fig. 3.. With these different configurations it is possible to evaluate the effect of the location in the thickness of the 1st ply drop from bottom to top of the specimen and also the effect of the orientation of this 1st ply drop either 45° or 0° ply. It shall be noted that a different material batch was used for the configuration v5, and the comparison of fatigue performance will be achieved with the v2 configuration of the same batch.

| *N°* | *8* | *7* | *6* | *5* | *4* | *3* | *2* | *1* | | |
|---|---|---|---|---|---|---|---|---|---|---|
| *20* | 90 | 90 | 90 | 90 | 90 | 90 | 90 | 90 | 90 | |
| *19* | 45 | 45 | 45 | 45 | 45 | 45 | 45 | 45 | 45 | |
| *18* | 0 | 0 | | | | | | | | x |
| *17* | 0 | 0 | 0 | 0 | 0 | 0 | 0 | 0 | 0 | |
| *16* | -45 | -45 | -45 | -45 | -45 | -45 | | | | x |
| *15* | 0 | 0 | 0 | 0 | 0 | 0 | 0 | 0 | 0 | |
| *14* | 45 | 45 | 45 | 45 | | | | | | x |
| *13* | 0 | 0 | 0 | 0 | 0 | 0 | 0 | 0 | | x |
| *12* | -45 | -45 | -45 | -45 | -45 | -45 | -45 | -45 | -45 | |
| *11* | 0 | 0 | 0 | 0 | 0 | 0 | 0 | 0 | 0 | |
| *10* | 0 | 0 | 0 | 0 | 0 | 0 | 0 | 0 | 0 | |
| *9* | -45 | -45 | -45 | -45 | -45 | -45 | -45 | -45 | -45 | |

| | | | | | | | | | | |
|---|---|---|---|---|---|---|---|---|---|---|
| *8* | 0 | 0 | 0 | 0 | 0 | 0 | 0 | | | x |
| *7* | 45 | 45 | 45 | | | | | | | x |
| *6* | 0 | 0 | 0 | 0 | 0 | 0 | 0 | 0 | 0 | |
| *5* | -45 | -45 | -45 | -45 | -45 | | | | | x |
| *4* | 0 | 0 | 0 | 0 | 0 | 0 | 0 | 0 | 0 | |
| *3* | 0 | | | | | | | | | x |
| *2* | 45 | 45 | 45 | 45 | 45 | 45 | 45 | 45 | 45 | |
| *1* | 90 | 90 | 90 | 90 | 90 | 90 | 90 | 90 | 90 | |

Fig. 2. Example of a configuration (v2) with all the ply-drops in grey

| | **v2** | | **v13** | | **v12** | | **v4** | | **v3** | | **v5** | |
|---|---|---|---|---|---|---|---|---|---|---|---|---|
| | 90 | | 90 | | 90 | | 90 | | 90 | | 90 | |
| | 45 | 90 | 45 | 90 | 45 | 90 | 45 | 90 | 45 | 90 | 45 | 90 |
| | 0 | 45 | 0 | 45 | 0 | 45 | 0 | 45 | 0 | 45 | 0 | 45 |
| | 0 | 0 | 0 | 0 | 0 | 0 | 0 | 0 | 0 | 0 | 0 | 0 |
| | 0 | 0 | 0 | 0 | 0 | 0 | 0 | 0 | 0 | 0 | 45 | 0 |
| | -45 | 0 | -45 | 0 | -45 | -45 | -45 | 0 | -45 | -45 | -45 | 45 |
| | 0 | -45 | 0 | -45 | 0 | 0 | 0 | -45 | 0 | 0 | 0 | -45 |
| | 0 | 0 | 0 | 0 | 0 | 0 | 0 | 0 | 0 | 0 | 0 | 0 |
| | -45 | 0 | -45 | 0 | -45 | -45 | -45 | 0 | -45 | -45 | -45 | 0 |
| | 0 | -45 | 0 | -45 | 0 | 0 | 0 | -45 | 0 | 0 | 45 | -45 |
| | 0 | 0 | 0 | 0 | 0 | 0 | 0 | 0 | 0 | 0 | 0 | 0 |
| | 0 | 0 | 0 | 0 | 0 | 0 | 0 | 0 | 0 | 0 | 0 | 0 |
| | 45 | 45 | 45 | 45 | 45 | 45 | 45 | 45 | 45 | 45 | 45 | 45 |
| | 90 | 90 | 90 | 90 | 90 | 90 | 90 | 90 | 90 | 90 | 90 | 90 |
| **No** | **2** | **1** | **2** | **1** | **2** | **1** | **2** | **1** | **2** | **1** | **2** | **1** |

Fig. 3. Location of 2nd and 1st ply-drops for the six configurations under study

### *2.2. Testing conditions and damage observation*

Under load, the asymmetry in the specimen geometry creates a bending moment which causes an out of plane deflection at the ply drop area. This may need to be controlled in order to be representative of the behaviour of an aeronautical composite panel, where boundary conditions may limit large out-of-plane deflection. The specimens were therefore clamped in an anti-deflection device and Teflon pads were inserted to minimise friction in the non-clamped zone (Fig. 4 ).The tests have been stopped regularly and both sides observed with an optical microscope in order to monitor the damages during fatigue loading,., Damage evolution has been filmed by a camera (60 images/s) on one side of the specimen during the last cycles before final failure.

## 3. FINITE ELEMENT MODELLING

A global-local 3D finite element models approach has been developed, with the code Samcef©, in order to calculate interlaminar stresses at ply drop areas. The local model is designed to correctly represent the free-edge and ply drop-off effects on the interlaminar stress distribution.

Fig. 4 Specimen clamped in the anti-buckling device

*3.1. Geometry and boundary conditions of the global-local model*

The global model represents the complete ply-drop zone plus the unclamped part of the laminates in the thick and the thin section, including the Teflon part of the anti-buckling device. To simulate the clamping condition, all degrees of freedom are restrained on both the right- and left-hand sides, except for the displacement in load direction on the latter. The laminate is modeled ply by ply with 20 nodes cubic elements, with one element per ply thickness. A contact condition without any friction has been imposed between the specimen and the anti-buckling device. The meshing in the width direction is refined in order to get cubic finite elements at free edges where stress gradient is the highest.

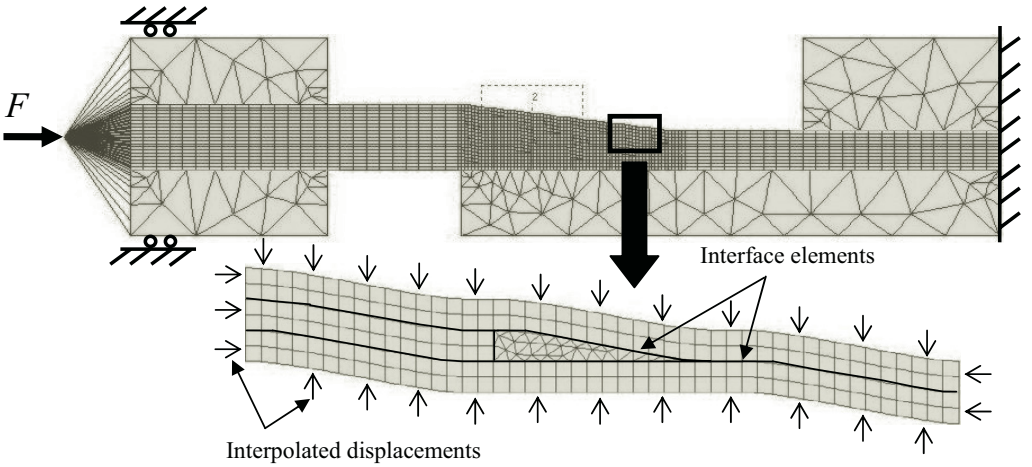


Fig. 5. Global (top) & local (bottom) finite element models for interlaminar stresses calculation

The local model represents a zone around a ply-drop, with one ply on the top and one ply on the bottom Thus, as many local models as ply-drops are analyzed. The displacements field obtained with the global model is imposed as a loading boundary condition on the local model. Interface elements are used to calculate the interlaminar stresses between consecutive plies. A mesh refinement study has shown that stress values are correctly represented with one element per ply for the global model, and 2 elements per ply for the local model by keeping elements cubic at the specimen edges. All material laws are linear elastic; the solver module is non-linear allowing for possible large deflections.

*3.2. Approach for calculation of representative values*

There are two main problems when calculating numerical stresses around ply-drops: namely the stress singularity at the dropped ply, and the edge-effect at the free edges. Convergence studies have shown that the average stress

values, calculated for a squared zone of 0.25 x 0.25 mm, converge for a mesh size of 2 elements per ply. With this approach it is possible to quickly and directly compare the stress values on both edges, in the middle and between different ply-drops. The colored mesh-grid (Fig. 6.) shows one of the zones of the interface elements used for calculating the average stress values.

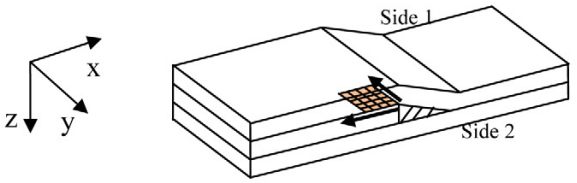


Fig. 6. Squared zone used to average interlaminar stresses near specimen's edges

## 4. RESULTS AND ANALYSIS

### *4.1. Static tests*

Repeats of four tests in tension and in compression have been done for the different configurations, with the exception of the v5 configuration due to a lack of material. It is noted that for all configuration tension strength is almost twice the compression one and that the failure is always catastrophic.

Table 1. Static strengths under tension and compression

| | Tension | | Compression | |
|---|---|---|---|---|
| Configuration | Average (MPa) | St.D. (MPa) | Average (MPa) | St.D. (MPa) |
| v2 | 819 | 46 | - 452 | 14 |
| v3 | 939 | 21 | - 508 | 30 |
| v4 | 922 | 24 | - 473 | 06 |
| v12 | 956 | 49 | - 509 | 08 |
| v13 | 867 | 37 | - 443 | 03 |
| All | *904* | *62* | *- 481* | *31* |

### *4.2. Fatigue tests*

Observations made during fatigue tests revealed that for all the configurations tested, the first significant damages are delaminations located at the first two ply drop-offs close to the thin part of specimens (Fig. 7. ). Other damages, such as transverse cracks of the two external plies oriented at 90° and 45°, were also observed but their importance appears as minimal when compared with the initiation and propagation of the delamination.

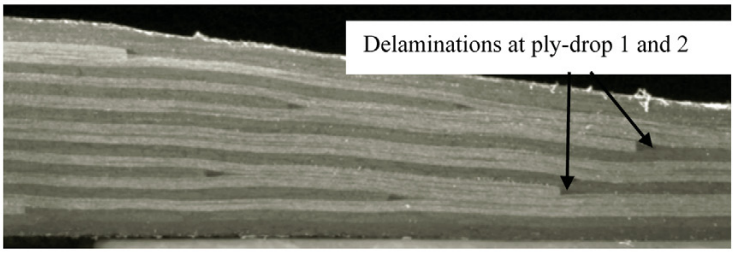

Fig. 7. Side 2 of v2 configuration tested at 50% and stopped at 10000 cycles with delaminations around ply-drop 1 and 2

Damage modes and locations have been identified by stopping the fatigue tests regularly and observing the two sides of the specimens. An asymmetrical distribution of delamination on the specimen's edges has been found, as shown in Fig. 8. for the 2nd ply-drop of the v4. It is to be noted that the delamination is visible on one side only (Side 2).

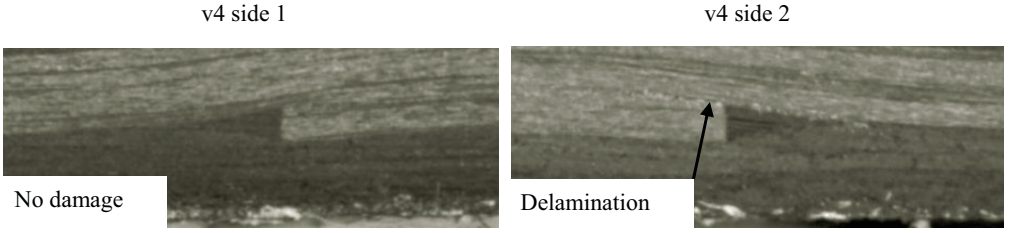


Fig. 8. Delamination at 2nd ply-drop of v4 tested at 50%, interrupted at 8000 cycles

The 3D global-local finite element model has been used to evaluate the interlaminar stresses close to the ply-drops. It has been shown that the stress distribution through the specimen width is non-symmetrical; with stresses being higher on one side than on the other.

Table 2. shows the frequency of delamination observed experimentally in fatigue tests, and the magnitude of the calculated interlaminar stresses averaged over a squared zone of 0.25 x 0.25 mm with the global-local model. Calculations were all performed for the compression load at static failure stress of the v2 configuration. The shear stresses in yz direction are small when compared with the other values and, being considered as negligible, are not presented.

Table 2. Frequency of delaminations observed in fatigue tests and calculated interlaminar stresses for the 2 first ply drops

| | Critical location | | | Side 1 (MPa) | | Side 2 (MPa) | |
|---|---|---|---|---|---|---|---|
| | PlyDrop | Side | Interface | $\sigma_{zz}$ | $\sigma_{xz}$ | $\sigma_{zz}$ | $\sigma_{xz}$ |
| v2 | 1 | 1 | 0°/0° | 34 | **98** | 33 | 57 |
| | 2 | 2 | -45°/0° | 38 | 24 | **61** | **103** |
| v3 | 1 | 2 | 0°/0° | 32 | 73 | 33 | **129** |
| | 2 | 2 | 0°/0° | **45** | -123 | 30 | **-138** |
| v4 | 1 | 2 | 0°/0° | **51** | -168 | 36 | **-198** |
| | 2 | 2 | 0°/0° | 27 | 81 | 29 | **134** |
| v12 | 1 | 1 | 0°/0° | 33 | 79 | 37 | **132** |
| v13 | 2 | 2 | 0°/0° | 25 | 74 | 29 | **117** |
| v5 | 1 | 2 | 45°/-45° | 56 | 47 | **66** | **-79** |

Side location of the first delamination

In bold Highest stress value ($\sigma_{zz}$ ou $\sigma_{xz}$)

It is important to notice that, for all the configurations, the side where delaminations initiate the most frequently during fatigue tests corresponds to the side where interlaminar stresses are the highest. Furthermore, on the preferred side of delamination initiation, the shear stress σxz is always higher than the opening stress σzz. This is observed for

all configurations except for v5 where the dropped ply is at 45° instead of 0°. For v5 configuration, shear stress and opening stress are of the same intensity.

*4.3. Criterion of delamination initiation*

To establish a basic (qualitative) criterion enabling us to predict delamination initiation at the edges of specimens some assumptions have been made. First of all, the material behavior is assumed to be linear without any damage. The critical delamination locations leading to the quasi-instantaneous failure of the specimen in static loading are supposed to be the same as the ones observed in fatigue.

The basic approach developed here is inspired from delamination onset criteria developed for free-edge delamination specimens [7-9]. It has been chosen to work with a quadratic interlaminar stress criterion where τ is the resultant of the two shear components (σxz and σyz). To deal with problems of singularity at free edges and close to ply-drops it has been chosen to average the stresses over a squared zone (due to the assumed isotropy of the interface). Identification of the criterion requires finding out the critical opening and shear stresses and the size of the zone used to average stresses.

$$\left(\frac{\overline{\sigma}_{zz}}{\sigma_{zz}^{rupture}}\right)^2 + \left(\frac{\overline{\tau}}{\tau^{rupture}}\right)^2 = 1 \qquad (1)$$

For each configuration, the interlaminar stresses fields were calculated for all the ply drop-offs at the compressive failure load of the configuration. The identification of the 3 criterion parameters was then performed by maximizing the number of critical points found out in a confidence interval, corresponding to the maximal standard deviation observed for the static strengths. As can be seen in Fig. 9 , most of the critical areas where delamination initiations lead to the brutal failure of the specimen under compressive static loading are correctly included inside the confidence interval.

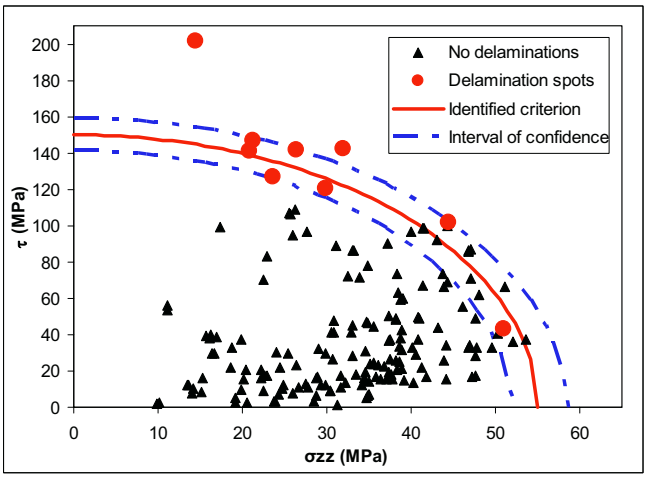


Fig. 9 Delamination initial criterion under static loading for all configurations

The parameters identified are presented in Table 3 . The distance needed to average stresses represents 1.5 times the elementary ply thickness which is consistent with literature data [7-8]. Interlaminar stresses are of correct order of magnitude, but the critical shear stress is clearly not representative of a typically expected value. This is certainly

due to the material linear assumption used to calculate the interlaminar stresses and this has to be addressed in the future. The criterion herein defined is semi-empirical and may be regarded as qualitative only.

Table 3 Identified criterion parameters

| a (mm) | σzz (MPa) | τ (MPa) |
|---|---|---|
| 0.375 | 55 | 150 |

*4.4. Damage evolution in fatigue*

Fig.10 presents the variation of total elongation vs cycle ratio to failure for the specimens cycled at 50% load level. For all configurations, the stiffness remains almost constant at the beginning of the fatigue life, up to a point where it starts to decrease steadily and to finally, close to the end of life, drop brutally. Damage evolution for the v2 and v4 configurations presents the most progressive evolution of stiffness during fatigue life. To identify the damage kinetics during fatigue one side of the specimen has been filmed. Observations show that there are three stages: a cycling without apparent damage, then delamination initiations with a stable propagation, slow or fast depending upon the configuration, and finally an unstable propagation very close to final failure.

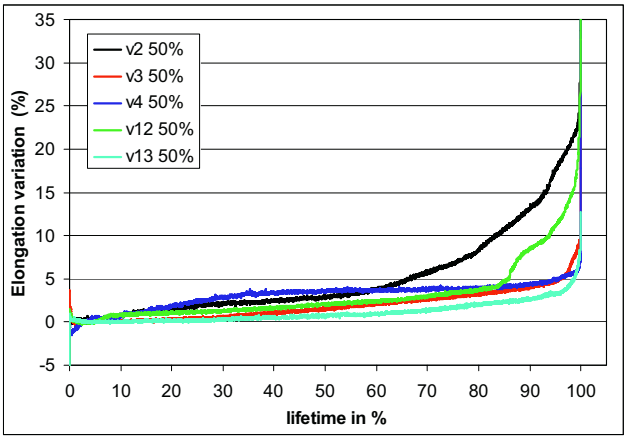


Fig.10 . Elongation variation for all configurations at 50% load level

Close to the final failure event, the films show that all the configurations are separated into three sub-laminates, resulting from the propagation of delaminations that initiated around 1st and 2nd ply-drops, propagating towards the thicker part of specimen. The number of continuous plies at 0° contained in these sub-laminates directly depends upon the 1st and 2nd ply-drop locations in the specimen thickness (see Table 4).

For all configurations, where the 1st and 2nd ply-drops are at 0°, stress/life curves comparison (Fig.11 ) shows the effect of ply-drop location has a fair effect on the fatigue behaviour. But there is no clear tendency concerning a precise effect of these locations. However, when comparing the effect of the orientation of 1st & 2nd ply drop on stress/life curves, (Fig. 12 ) it is seen that it may be beneficial for fatigue performance to first stop disoriented plies at 45°, rather than plies at 0°.

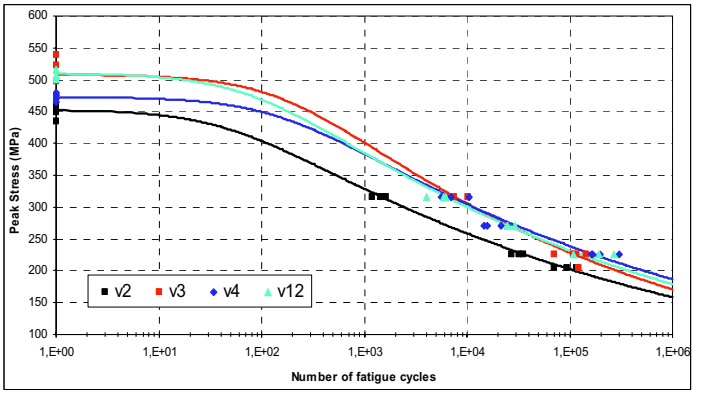


Fig.11 Stress/life curves for configurations with 1st & 2nd ply drops at 0°

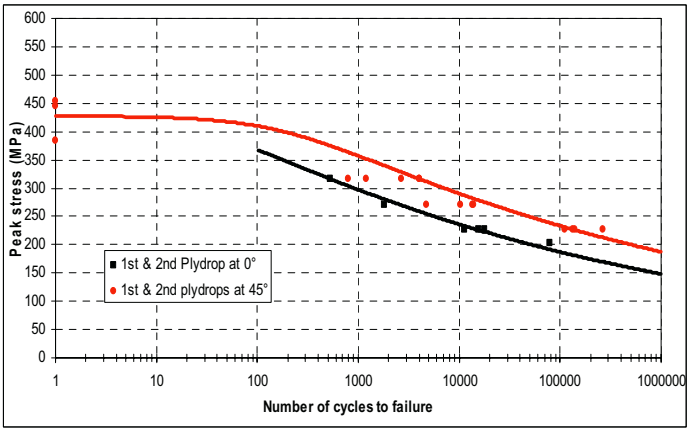


Fig. 12 Comparison of Stress/life curves for configuration with 1st & 2nd ply drops at 0° (v2) and at 45° (v5)

It was observed that the location in the thickness of the 1st and 2nd ply-drops at 0°, where delaminations initiate first, determines the number of plies at 0° in the sub-laminates created by the delaminations propagation. And this parting of laminates seems to have an effect on the fatigue performance. The larger the number of 0° plies per sub-laminate, the longer the lifetime (see Table 4).

Table 4 Number of plies at 0° per sublaminate compared to Nf at 50% of load level for each configuration

| N° of Sub-laminate | v2 | v13 | v3 | v12 | v4 |
|---|---|---|---|---|---|
| 1 | 2 | 1 | 4 | 1 | 0 |
| 2 | 2 | 3 | 1 | 4 | 6 |
| 3 | 2 | 1 | 1 | 1 | 0 |
| Average Nf (at 50%) | 31600 | 50000 | 111000 | 190000 | 207260 |

## 5. Conclusions and perspectives

A specific tapered highly oriented composite laminate has been defined with 8 ply-drops. Several specimen configurations with different positions of ply-drops in the thickness direction have been tested, under static and fatigue loading at R=-1.

Static tests have shown that compressive loading is much more critical than tension. Catastrophic failure does not allow the identification of the static damage process. However, observations during cyclic loading have shown that delaminations firstly initiate around the 1st and 2nd ply-drops the closest to the thin side part of specimen. Furthermore, delamination initiates preferably on one side of specimens depending upon the configuration and the ply-drop. A 3D global-local FE model has been developed to calculate the interlaminar stresses due to both free-edge effects and ply-drop effects. Comparing the experimental observations with the numerical values shows that the side with the highest frequency of delamination damage corresponds to the side with the highest interlaminar stresses. A semi-empirical interlaminar stress criterion has then been evaluated to predict the delamination initiation leading to the static failure of the different configurations.

Damage evolution during fatigue was observed and follows a three stage process: namely, a cycling without damage, then delamination initiations with a stable propagation, slow or fast depending upon the configuration, and finally an unstable propagation very close to final failure. Stress/life curves have shown that ply drops design configurations have a relatively effect on the fatigue life. For instance, it may be beneficial to drop the ply with a 45° orientation first. Furthermore, it has been observed that the propagation of initial delaminations separate the laminate into three sub-laminates depending on the 1st and 2nd ply-drops location. The number of 0° plies inside these sub-laminates presents a clear relation with the fatigue life, giving an idea of the key role played by ply-drop locations on fatigue behaviour of tapered laminate.

## References

[1] G. B. Murri, J. R. Schaff, A. L. Dobyns, Fatigue and damage tolerance analysis of a hybrid composite tapered flexbeam . American Helicopter Soc. 57th Forum 2001, http://search.nasa.gov

[2] D. J. Shim, Role of delamination and interlaminar fatigue in the failure of laminates with ply dropoffs. PhD Thesis; 2002, MIT (USA).

[3] C. A. Steeves, N. A. Fleck, Compressive strength of composite laminates with terminated internal plies. Composites: Part A, 2004, p.1-8

[4] O. T. Thomsen, F. Mortensen, Y. Frostig, Interface failure at ply drops in CFRP/sandwich panels . J. of Composite Materials, 2000; 34, p.135-157

[5] A. Mukherjee, B. Varughese, Design guidelines for ply drop-off in laminated composite structures . Composites Part B, 2001, 32, p.153-164

[6] R. Ganesan, D. Y. Liu, Progressive failure and post-buckling response of tapered composite plates under uni-axial compression, Composite Structures, 82, p.159-176, 2007

[7] L lagunegrand et al., Initiation of free-edge delamination in composite laminates, Composites Science ans Technology, 2006, 66 p.1315-1327

[8] T. Lorriot et al., Onset of free-edge delamination in composite laminates, Composites: Part B, 2003, 34 p.459-471

[9] J.C. Brewer, P.A. Lagace, Quadratic stress criterion for initiation of delamination, J. of Composite Materials; 1988, 22, p.1141-1155